Molecules and Cells

Icariside II Promotes the Differentiation of Adipose Tissue-Derived Stem Cells to Schwann Cells to Preserve Erectile Function after Cavernous Nerve Injury

Tao Zheng, Tian-biao Zhang, Chao-liang Wang, Wei-xing Zhang, Dong-hui Jia, Fan Yang, Yang-yang Sun, Xiao-ju Ding, and Rui Wang*

Department of Andrology, Institute of Andrology, The First Affiliated Hospital of Zhengzhou University, Zhengzhou, 450052, China
*Correspondence: zhengtao-335@163.com
http://dx.doi.org/10.14348/molcells.2018.2236
www.molcells.org

Icariside II (ICA II) is used in erectile dysfunction treatment. Adipose tissue-derived stem cells (ADSCs) are efficient at improving erectile function. This study aimed to explore the action mechanism of ADSCs in improving erectile function. ADSCs were isolated from the adipose tissues of rats. Cell proliferation was determined using the Cell Counting Kit-8 (CCK-8) assay. The expressions of mRNA and protein were determined separately through qRT-PCR and western blot. The endogenous expressions of related genes were regulated using recombinant plasmids and cell transfection. A Dual-Luciferase Reporter Assay was performed to determine the interaction between miR-34a and STAT3. Rat models with bilateral cavernous nerve injuries (BCNIs) were used to assess erectile function through the detection of mean arterial pressure (MAP) and intracavernosal pressure (ICP). ICA II promoted ADSCs' proliferation and differentiation to Schwann cells (SCs) through the inhibition of miR-34a. Suppressed miR-34a promoted the differentiation of ADSCs to SCs by up-regulating STAT3. ICA II promoted the differentiation of ADSCs to SCs through the miR-34a/STAT3 pathway. The combination of ICA II and ADSCs preserved the erectile function of the BCNI model rats. ADSCs treated with ICA II markedly preserved the erectile function of the BCNI model rats, which was reversed through miR-34a overexpression. ICA II promotes the differentiation of ADSCs to SCs through the miR-34a/STAT3 pathway, contributing to erectile function preservation after the occurrence of a cavernous nerve injury.

Keywords: ICA II, ADSCs, erectile function, miR-34a, STAT3

INTRODUCTION

Erectile dysfunction (ED) is a disease partially caused by cavernous nerve injury and usually afflicts men aged 40 years and older. It often endangers the physical and psychological health of its patients (Shamloul and Ghanem, 2013). Icariin (ICA) is clinically used as a traditional Chinese medicine for ED treatment, and ICA II is the main metabolite of ICA following its oral administration (Cao et al., 2012). ICA and ICA II can be isolated from herba epimedii and are useful in treating ED, which may be attributed to their effects on nitric oxide synthase (NOS) activity (Liu et al., 2011). Nitric oxide (NO) is an important neurotransmitter that plays a decisive role in the process of erection, and NO generated by neuronal NOS (nNOS) is considered the main factor responsible

Received 22 September, 2017; revised 6 March, 2018; accepted 25 March, 2018; published online 14 June, 2018

eISSN: 0219-1032

for the immediate relaxation of the corpus cavernosum (Amany and Heba, 2013). nNOS is an indispensable enzyme related to NO production that thereby modulates penile vascular homeostasis, and a reduction of nNOS expression usually leads to circulatory and structural changes in penile tissues, resulting in ED (Musicki et al., 2009).

ADSCs are a population of multi-potent stem cells that can differentiate into several other types of cells and can be easily harvested from adipose tissue, making them the most promising stem cells for clinical therapy (Zuk, 2010). Recently, ADSCs-based therapy has been considered as a potential alternative for nerve damage prevention (Jeong et al., 2013), and ADSCs have been demonstrated to ameliorate cavernous nerve injury-associated ED (Yang et al., 2015). Furthermore, ADSCs can be induced to differentiate into Schwann-like cells, one of the ideal alternative cell systems for SC generation (Gao et al., 2015b). SCs are principal glia of the peripheral nervous system that play a pivotal function in repairing nervous injury, including cavernous nerve injury and subsequent ED (Wang et al., 2015). The S100β, the glial fibrillary acidic protein (GFAP), and P75 are specific known markers of SCs that are often used for SC differentiation studies.

MicroRNAs (miRNAs) refer to a group of endogenous noncoding RNAs that negatively regulate gene expression and play a crucial role in modulating the differentiation of ADSCs (Chen et al., 2014). The miR-135 and miR-26a have been identified as regulators of the osteogenic differentiation of ADSCs (Su et al., 2015; Xie et al., 2016). MiR-34a inhibits the differentiation of human ADSCs by regulating cell cycle and senescence induction (Park et al., 2015), and it also inhibits STAT3 expression (Li et al., 2015). Additionally, adipose-derived mesenchymal SCs promote osteosarcoma proliferation and metastasis by activating the STAT3 pathway (Wang et al., 2017). The above findings suggest that the miR-34a/STAT3 pathway may play a vital role in the differentiation of ADSCs.

In addition, the action mechanism of ICA II in ameliorating ED appears to be associated with enhanced endogenous SC differentiation (Xu et al., 2015). ICA II also has been proven to promote the osteogenic differentiation of canine bone marrow mesenchymal stem cells (BMSCs) through the PI3K/AKT/mTOR/S6K1 signaling pathway (Luo et al., 2017). ADSCs are similar to BMSCs in differentiation and protein secretion (Yang et al., 2015); hence, we speculated that ICA II may relieve ED by promoting the differentiation of ADSCs to SCs, which may be associated with the miR-34a/STAT3 pathway. We undertook this study to explore the action mechanism of ICA II and ADSCs in preserving erectile function, and the role of the miR-34a/STAT3 pathway in this process.

MATERIALS AND METHODS

Isolation and culture of ADSCs

All animal experiments were approved by the Ethics Committee of the First Affiliated Hospital of Zhengzhou University, and performed according to the National Institutes of Health Guidelines for the Care and Use of Laboratory Animals.

SD male rats (weighing 60-70g and at 3 weeks old) were purchased from the Laboratory Animal Center of Zhengzhou University and sacrificed, and their adipose tissues were isolated from their bilateral groins. The adipose tissue was incubated in 0.1% collagenase Type I (Gibco) for 50 min at 37℃ and shaken for 30 s after every 15 min. After centrifugation at 250 g for 10 min at room temperature, the adipose stromal vascular fraction (SVF) was treated with a red blood cell lysis buffer (160 mM NH4Cl) for 10 min at 4℃. After being centrifuged and rinsed with PBS, the remaining cells were resuspended in a DMEM/F12 medium supplemented with 10% fetal bovine serum (FBS, Gibco) and cultured at 37℃ with 5% CO_2. ADSCs passaged up to the third passage were used in this study.

Cell proliferation assay

Cell proliferation was determined using a Cell Counting Kit-8 (CCK-8, Sigma) assay. The ADSCs at the third passage were seeded in 24-well plates at 1×10^4 cells/well for 24 h, then treated with the solution containing ICA II (Tauto Biotech) at different concentrations (10^{-9}-10^{-5} mol/L). The cells cultured in the complete medium served as a control. Cell proliferation was determined both at 48 h and 96 h. ADSCs were treated with a CCK-8 reagent with 10 μl in each well for 4 h, and the absorbance at 450 nm was measured using a microplate reader (Bio-Rad).

Differentiation of ADSCs into SCs

ADSCs at the third passage were dissociated and cultured in the DMEM medium with 1 mM β-mercaptoethanol and 10% FBS at 37℃ with 5% CO_2 for 24 h. The cells were washed with PBS and the medium was replaced with fresh DMEM with 10% FBS and 35 ng/ml all-trans-retinoic acid, maintained at 37℃ with 5% CO_2 for 72 h. Next, the cells were washed with PBS and the medium was replaced with fresh DMEM containing 10% FBS, 5 mmol/L forskolin (Sigma), 10 ng/ml basic Fibroblast Growth Factor (bFGF, Sigma), 10 ng/ml platelet-derived growth factor (PDGF, Sigma), and 200 ng/ml recombinant human heregulin-β1 (Sigma). It was cultured at 37℃ with 5% CO_2 for 7 days. The normal SCs separated from the rats served as a control.

Quantitative real-time PCR (qRT-PCR)

The ADSCs and SCs were treated with a TRIzol reagent (Invitrogen) for the total RNA extraction. A cDNA Reverse Transcription Kit (ABI) was used in the reverse transcription for the cDNA synthesis. A qRT-PCR was conducted with the SYBR Select Master Mix (ABI) on an ABI 7300Fast Real-Time PCR system. The primers were designed and synthesized by Sangon Biotech (China). The relative expression was calculated using the $2^{-\Delta\Delta Ct}$ method.

Western blotting

Western blotting was carried out to analyze protein expression. Briefly, the proteins were separated using SDS-PAGE with an electrophoresis system and transferred onto the polyvinylidene difluoride (PVDF) membrane (Bio-Rad). The membrane was then blocked with 5% skimmed milk for 1 h at RT, then incubated with primary antibodies including the

anti-S100β antibody (Abcam, 1:1000); the anti-GFAP antibody (Abcam, 1:2000); the anti-P75 antibody (Abcam, 1:1000); the anti-STAT3 antibody (Abcam, 1:500); and the anti-β-actin antibody (Abcam, 1:1000) at 4℃ overnight. Next, the membrane was incubated with HRP-bound antibodies at RT for 1 h, and the target proteins were visualized through ECL Plus Western Blotting Substrate (Thermo Fisher).

Cell transfection

The miR-34a mimic (No. miR10000815-1-5) and miR-34a inhibitor (No. miR20000815-1-5) were purchased from RiboBio (Guangzhou) and transfected into the cells using Lipofectamine 2000 (Invitrogen) according to the instructions. The efficiency of the cell transfection was examined through a qRT-PCR analysis.

Dual-Luciferase Reporter Assay

The WT STAT3 3'-UTR or MUT IL-10 3'-UTR were inserted into the pmirGLO vector (Promega). Then the vectors and miR-34a mimic (or its negative control, pre-NC) or miR-34a inhibitor (or its negative control, NC) were co-transfected into the ADSCs using Lipofectamine 2000 (Invitrogen). Luciferase activity was detected by the dual Luciferase Reporter Assay System (Promega), according to the manufacturer's specifications.

Construction of the rat model with bilateral cavernous nerve injury (BCNI)

Adult male SD rats (weighing 250-300 g and aged 8-10 weeks) were divided into six groups: sham (n = 6), BCNI (n = 6), PBS (n = 6), ADSCs (n = 6), ICA II (n = 6), and ICA II+ADSCs (n = 6). The BCNI model was established as previously reported (Chen et al., 2016b). In brief, the rats were anesthetized with pentobarbital sodium (40 mg/kg) through intraperitoneal injection. The rats were subsequently fixed onto a heated surgical table in a supine position. After being shaved and iodinated for sterilization, an incision at the lower abdominal midline was made, to expose the prostate glands. In the sham group (n = 6), the abdomen was then closed. The major pelvic ganglion (MPG) and cavernous nerve were exposed on either side of the prostate, and the BCNI model (n = 6) was induced via the direct perturbation of the nerve 5 mm distal to the MPG using mosquito hemostatic forceps for 1 min. After the penis was exposed, an elastic band was applied to the base of the penis and maintained for 2 min, and a 1×10^6 rat ADSC (Passage 3) suspension in 0.2 ml PBS (ADSCs, n = 6) or 0.2 ml PBS alone (PBS, n = 6) was injected into both corpora cavernosa. An ICA II (4.5 mg/kg/day) treatment was performed with intragastric administration to the ICA II (n = 6) and ICA II+ADSCs (n = 6) groups.

Erectile function evaluation

The erectile function of the rats was evaluated with mean arterial pressure (MAP) and intracavernosal pressure (ICP) four weeks after the surgery and injection as previously described (Ouyang et al., 2014). Each rat was anesthetized with pentobarbital sodium (40 mg/kg) through intraperitoneal injection. With a cervical median incision made, the left carotid artery was subsequently cannulated with a PE-50 catheter filled with a 250 IU/ml heparin solution for MAP (mmHg) measurement. A 25G needle was inserted into one side of the corpus cavernosum and connected to another pressure transducer for the ICP (mmHg) detection. With a midline laparotomy, the cavernosal nerve was identified and isolated, and a bipolar hook electrode attached to a signal generator (BL-420F, China) was placed around the left cavernous nerve for continuous stimulation. The monophasic rectangular pulses were recorded and analyzed. Erectile function was evaluated with the ratio of ICP /MAP. The penis was then harvested for qRT-PCR and western blot analyses.

Overexpression of miR-34a in rats

The ADSCs were transfected with an miR-34a mimic (dADSC+miR-34a) by Lipofectamine 2000 (Invitrogen), then treated with ICA II and cultured for differentiation induction. With the dADSC+NC or dADSC+miR-34a injections, BCNI model rats were divided into three groups: BCNI (n = 6), BCNI+dADSC+NC (n = 6), and BCNI+dADSC+miR-34a (n = 6) groups. ICP and the ratio of ICP/MAP were detected four weeks after the injection.

Statistical analysis

All statistical analyses in this study were performed using SPSS 22.0 software (SPSS Inc.). Quantified data were expressed with mean ± standard deviation, and the differences between groups were examined by Student's *t* tests. Multiple comparisons among groups were conducted by using one-way analysis of variance (ANOVA) followed by Student-Newman-Keuls post hoc tests. A value of $P < 0.05$ was considered statistically significant.

RESULTS

ICA II promoted ADSCs' proliferation and differentiation into SCs

The results of the cell proliferation detection revealed that ICA II significantly promoted the proliferation of ADSCs, both for the 48 h (D2) and 96 h (D4) treatments (Fig. 1A). In the process of the ADSCs' differentiation into SCs, the cells were treated with ICA II for 72 h, and the morphology of the ADSCs and the SCs' differentiation from the ADSCs is displayed in Figs. 1B and 1C, respectively. The expression of S100β and GFAP in the SCs differentiated from the ADSCs was also confirmed using the immunofluorescence staining method (Figs. 1D and 1E). The percentage of $S100\beta^+GFAP^+$ cells was clearly elevated by ICA II in the process of differentiation from the ADSCs to the SCs (Fig. 1F). In the process of the ADSCs' differentiation into SCs, the mRNA level of S100β, GFAP, and P75 was markedly increased (Fig. 1G), and their protein levels were also boosted with the ICA II treatment (Fig. 1H). A higher concentration of ICA II showed more remarkable stimulation effects on the proliferation and differentiation of ADSCs to SCs.

ICA II promoted the differentiation of ADSCs to SCs through the inhibition of miR-34a

After treatment with ICA II (10^{-5} mol/L) for 48 h and induced

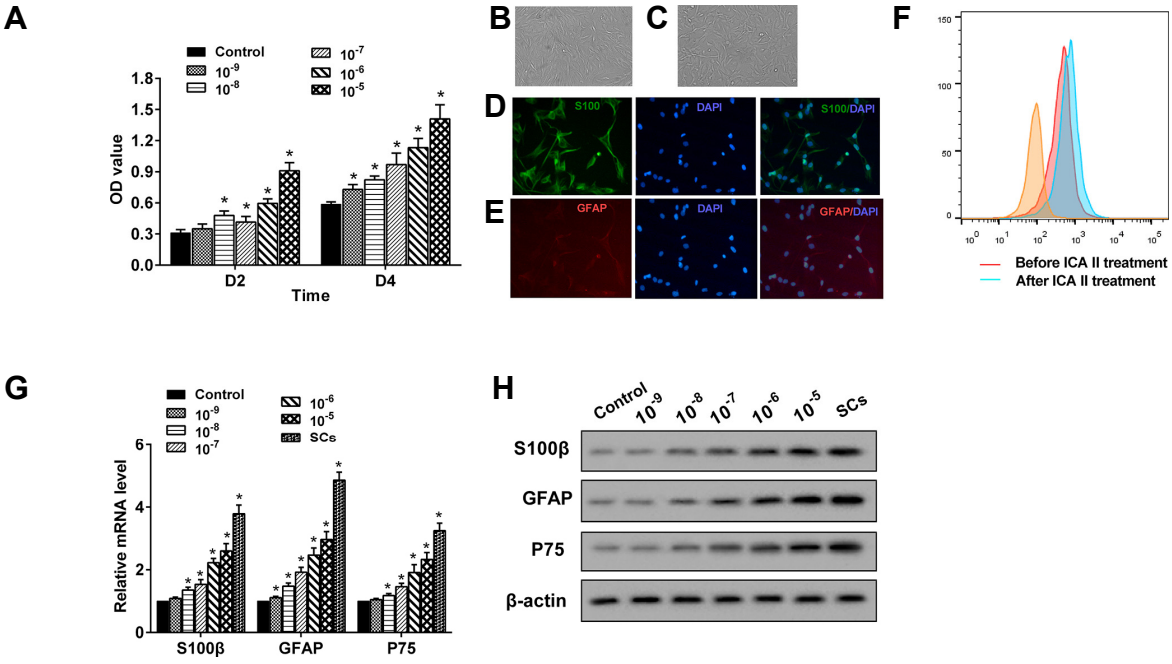

Fig. 1. ICA II promoted ADSCs' proliferation and differentiation into SCs. (A) ADSCs were treated with ICA II with a concentration of 10^{-9}-10^{-5} mol/L and cell proliferation was determined through a CCK-8 assay at 48 h (D2) and 96 h (D4), respectively. *P < 0.05 vs. control. (B, C) After treatment with ICA II for 72 h, the morphology of ADSCs and the SCs differentiated from the ADSCs were obtained using a microscope (400×). (D, E) The expression of S100β and GFAP in the Schwann cells differentiated from the ADSCs was also confirmed by using the immunofluorescence staining method. (F) The percentage of $S100\beta^{+}GFAP^{+}$ cells was clearly elevated by ICA II in the process of differentiation from ADSCs to Schwann cells. (G) The mRNA levels of S100β, GFAP, and P75 in the ADSCs were quantified using qRT-PCR. *P < 0.05 vs. control. (H) The expression of S100β, GFAP, and P75 proteins was analyzed through Western blot.

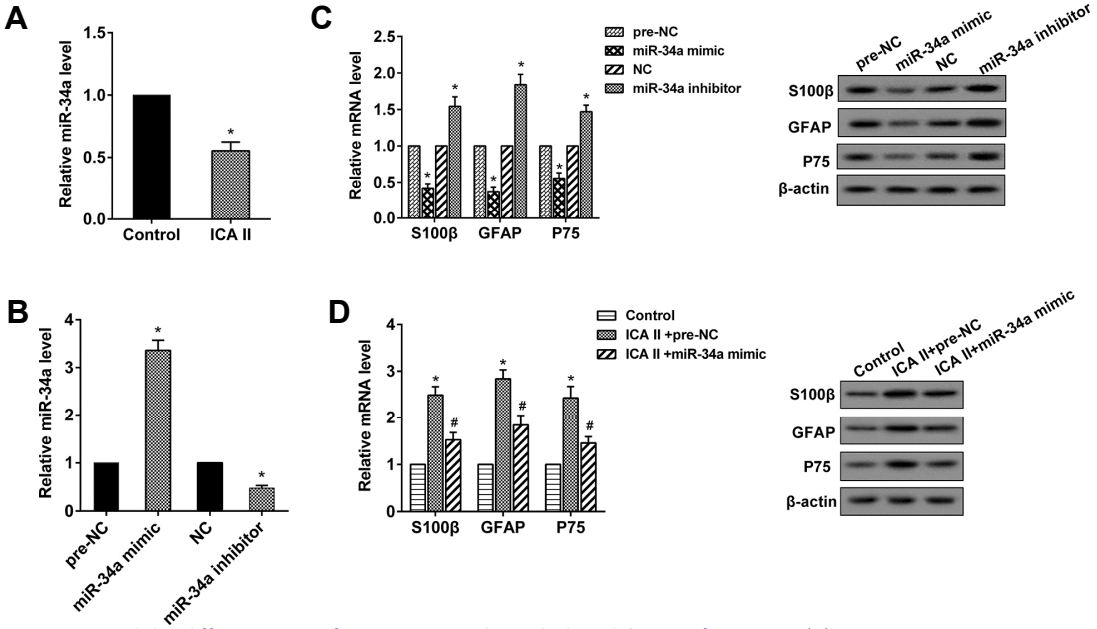

Fig. 2. ICA II promoted the differentiation of ADSCs to SCs through the inhibition of miR-34a. (A) The miR-34a level was determined using qRT-PCR. *P < 0.05 vs. control. (B) The miR-34a level was determined using qRT-PCR. *P < 0.05 vs. pre-NC. *P < 0.05 vs. NC. (C) The expression levels of S100β, GFAP, and P75 mRNA and protein were analyzed through qRT-PCR and western blot, respectively. *P < 0.05 vs. pre-NC. *P < 0.05 vs. NC. (D) The expression levels of S100β, GFAP and P75 mRNA and protein were analyzed through qRT-PCR and Western blot, respectively. *P < 0.05 vs. control. # P < 0.05 vs. ICA II+pre-NC.

SC differentiation, the expression of miR-34a in the ADSCs declined (Fig. 2A). With the miR-34a mimic transfected, the miR-34a level was up-regulated in the ADSCs, which was reversed through miR-34a inhibitor transfection (Fig. 2B). The up-regulation of miR-34a suppressed the expression of the mRNAs and proteins of S100β, GFAP, and P75, while the down-regulation of miR-34a reversed this situation (Fig. 2C). The miR-34a mimic reversed the promoting effect of ICA II on the expression of the mRNAs and proteins of S100β, GFAP, and P75 (Fig. 2D), suggesting that the over-expressed miR-34a reversed the promoting effect of ICA II in the differentiation of ADSCs to SCs.

MiR-34a negatively regulated STAT3, and STAT3 promoted the differentiation of ADSCs to SCs

The binding sites between miR-34a and the 3'UTR of STAT3 were analyzed using the bioinformatics method (microrna.org) (Fig. 3A). The results of the Dual-Luciferase Reporter Assay showed that the miR-34a mimic obviously suppressed the luciferase activity of the 3'-UTR of the STAT3 wild-type (WT), which was completely reversed by the miR-34a inhibitor. Meanwhile, the luciferase activity of the 3'-UTR of the STAT3 mutant (MUT) was not affected by the miR-34a mimic or inhibitor (Fig. 3B). The data indicated that miR-34a targets the 3'-UTR of STAT3. The miR-34a mimic decreased the expression of STAT3 mRNA and protein in ADSCs, while the miR-34a inhibitor did just the opposite (Fig. 3C). The STAT3 mRNA and protein were up-regulated in the ADSCs treated by ICA II (Fig. 3D) and with pcDNA-STAT3 transfection (Fig. 3E). The pcDNA-STAT3 also increased the expression of S100β, GFAP, and P75 mRNA and proteins (Fig. 3F). The si-STAT3 repressed the expression of STAT3 in

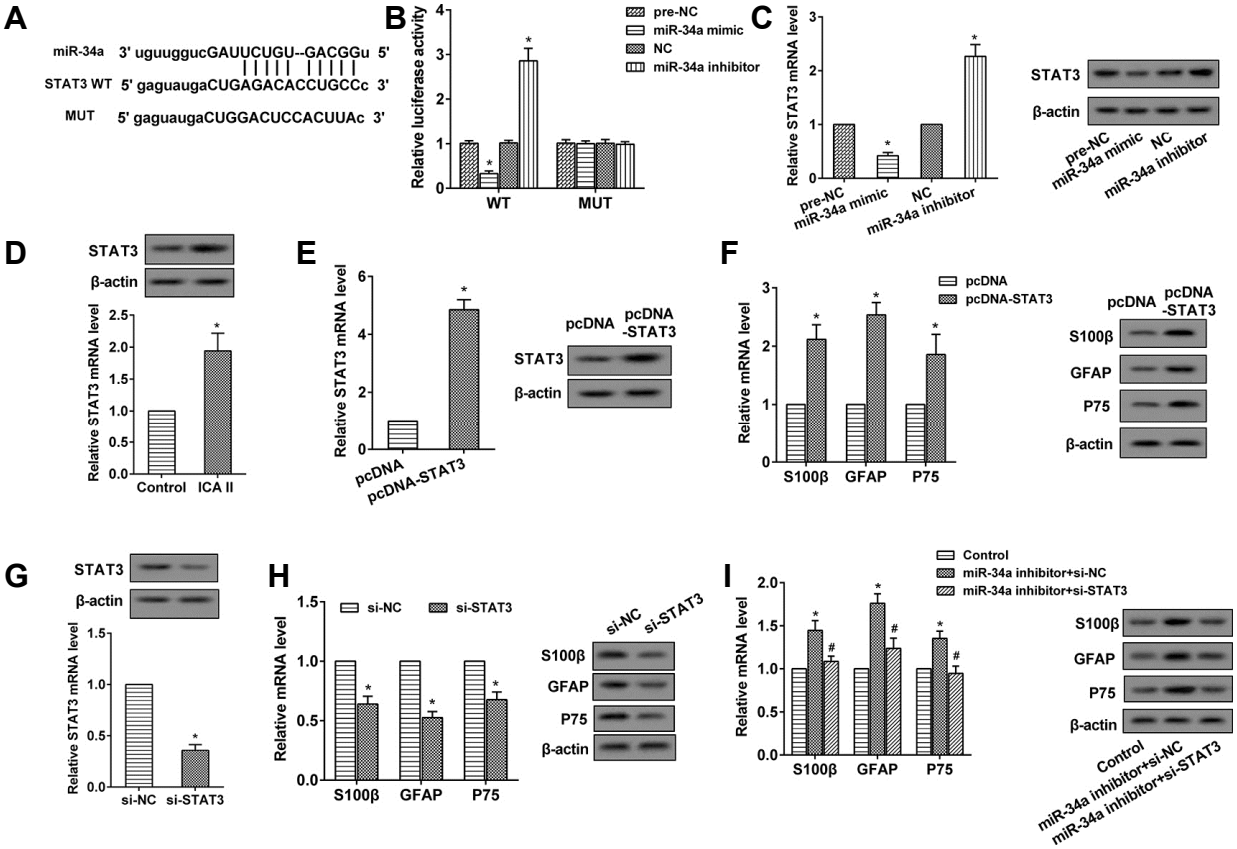

Fig. 3. MiR-34a negatively regulated STAT3, and STAT3 promoted the differentiation of ADSCs to SCs. (A) The binding sites between miR-34a and STAT3 were predicted using microrna.org. (B) Luciferase activity was detected to demonstrate the interaction between miR-34a and STAR3. *P < 0.05 vs. pre-NC. *P < 0.05 vs. NC. (C) The expression levels of STAT3 mRNA and protein were analyzed using qRT-PCR and western blot, respectively. *P < 0.05 vs. pre-NC. *P < 0.05 vs. NC. (D) The expression levels of STAT3 mRNA and protein were analyzed using qRT-PCR and western blot, respectively. *P < 0.05 vs. control. (E) The expression levels of STAT3 mRNA and protein were analyzed using qRT-PCR and western blot, respectively. *P < 0.05 vs. pcDNA. (F) The expression levels of S100β, GFAP, P75 mRNA, and protein were analyzed using qRT-PCR and Western blot, respectively. *P < 0.05 vs. pcDNA. (G) The expression levels of STAT3 mRNA and protein were analyzed using qRT-PCR and Western blot, respectively. *P < 0.05 vs. si-NC. (H) The expression levels of S100β, GFAP, P75 mRNA and protein were analyzed using qRT-PCR and western blot, respectively. *P < 0.05 vs. si-NC. (I) The expression levels of S100β, GFAP, P75 mRNA, and protein were analyzed by qRT-PCR and Western blot, respectively. *P < 0.05 vs. control. # P < 0.05 vs. miR-34a inhibitor+si-NC.

the ADSCs (Fig. 3G), and it also inhibited the expression of S100β, GFAP, and P75 mRNA and proteins (Fig. 3H). The si-STAT3 reversed the promoting effect of the miR-34a inhibitor on the expression of S100β, GFAP, and P75 mRNA and proteins (Fig. 3I), implying that si-STAT3 reversed the promoting effect of the miR-34a inhibitor in the differentiation of ADSCs to SCs.

ICA II promoted the differentiation of ADSCs to SCs through the miR-34a/STAT3 pathway

The ADSCs were placed into 4 groups: control; ICA II+pre-NC+pcDNA (transfected with pre-NC and pcDNA, and treated with ICA II); ICA II+miR-34a mimic+pcDNA (transfected with the miR-34a mimic and pcDNA, and treated with ICA II); and ICA II+miR-34a mimic+pcDNA-STAT3 (transfected with the miR-34a mimic and pcDNA-STAT3, and treated with ICA II). The expression of mRNA and proteins of S100β, GFAP, and P75 were observed. It was suggested that the positive regulation of ICA II on ADSC differentiation was reversed by the miR-34a mimic, and was further reversed by pcDNA-STAT3 (Figs. 4A and 4B). It can be summarized that ICA II promoted the differentiation of ADSCs to SCs through the miR-34a/STAT3 pathway.

Combination of ICA II and ADSCs preserved the erectile function of the BCNI model rats

Four weeks after the ADSCs injection, the erectile function of adult male SD rats in six groups (n = 6 in each group) was assessed with an ICP value and ICP/MAP ratio, and the expression of nNOS and S100β in the penile tissue was also detected. It showed that both ADSCs and ICA II significantly increased the ICP value and ICP/MAP ratio, as did the combined use of ADSCs and ICA II (Figs. 5A and 5B). The expression of nNOS and S100β in the penile tissue was obviously promoted by ADSC and ICA II treatment solely, and by the combined use of ADSCs and ICA II (Fig. 5C). These findings indicated that the combination of ICA II and ADSCs preserved the erectile function of the BCNI model rats.

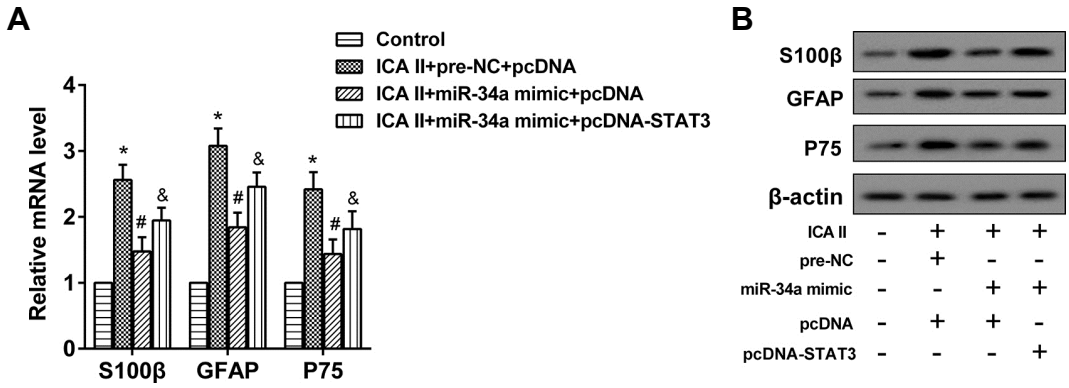

Fig. 4. ICA II promoted the differentiation of ADSCs to SCs through the miR-34a/STAT3 pathway. (A) The expression levels of S100β, GFAP, and P75 mRNA were analyzed using qRT-PCR. *P < 0.05 vs. control. # P < 0.05 vs. ICA II+pre-NC+pcDNA. &P<0.05 vs. ICA II+miR-34a mimic+pcDNA. (B) The expression levels of S100β, GFAP, and P75 protein were analyzed using Western blot.

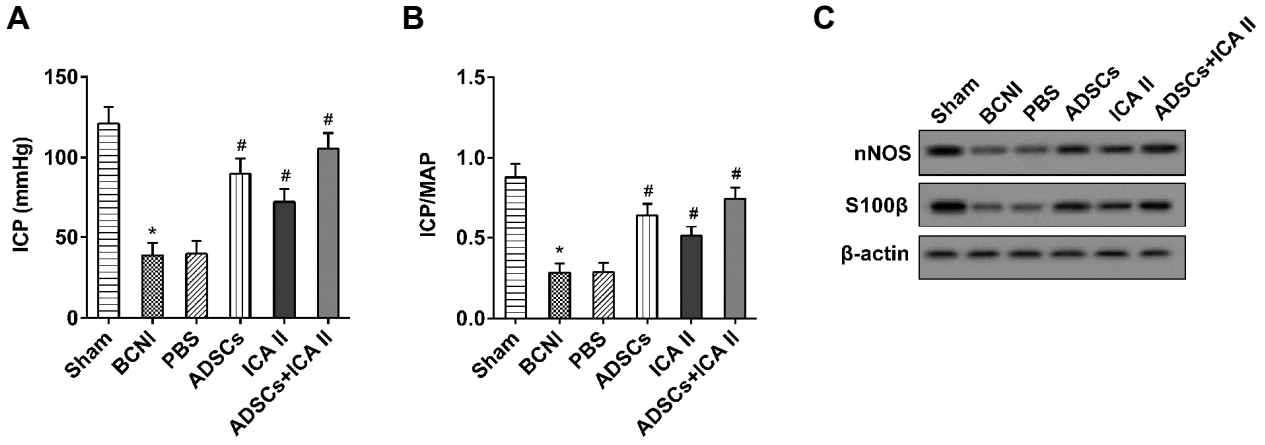

Fig. 5. A combination of ICA II and ADSCs preserved the erectile function of BCNI model rats. (A, B) The ICP and ICP/MAP were detected to evaluate the erectile function of the BCNI model rats. *P < 0.05 vs. sham. # P < 0.05 vs. PBS. (C) The expression levels of S100β, GFAP, and P75 protein were analyzed using Western blot.

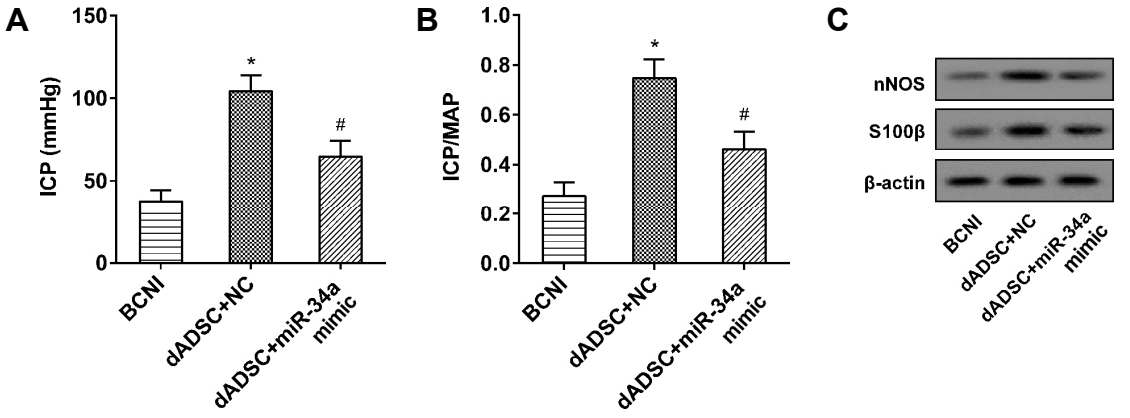

Fig. 6. The influence of miR-34a on the therapeutic effect of ADSCs on erectile function preservation of BCNI model rats. (A, B) The ICP and ICP/MAP were detected to evaluate the erectile function of the BCNI model rats. $*P < 0.05$ vs. BCNI. $^{\#}P < 0.05$ vs. dADSC+NC. (C) The expression levels of S100β, GFAP, and P75 protein were analyzed using Western blot.

Influence of miR-34a on the therapeutic effect of ADSCs on preserving erectile function in BCNI model rats

Four weeks after the ADSCs' (treated with ICA II) injection, the erectile function of the BCNI model rats in three groups (n = 6 in each group) was assessed with an ICP value and ICP/MAP ratio, and the expression of nNOS and S100β in the penile tissue was also determined. The ICP value and ICP/MAP ratio were sharply elevated by dADSC (ADSCs treated with ICA II), and the nNOS and S100β were also up-regulated, while the role of dADSC was significantly reversed by the overexpression of miR-34a (Figs. 6A-6C). The results implied that erectile dysfunction in the BCNI model rats was evidently ameliorated by dADSC, but reversed by miR-34a overexpression.

DISCUSSION

In this study, the influence of ICA II, miR-34a and STAT3 on the differentiation of ADSCs to SCs was investigated, and their role in the preservation of erectile function was confirmed. It can be concluded that ICA II promotes the differentiation of ADSCs to SCs through the miR-34a/STAT3 pathway, contributing to erectile function preservation after a cavernous nerve injury. This is the first time that the role of ICA II in ADSC differentiation was demonstrated and the mechanism of ICA II in preserving erectile function was elucidated, offering a significant theoretical basis for the utilization of ICA II for ED treatment. The findings also provide a reference for the treatment of other diseases related to nerve injuries.

ICA and ICA II are the active components of the traditional Chinese medicine herba epimedii, and are widely used in treating sexual dysfunction, osteoporosis, and inflammatory disease, showing various neuroprotective and anti-inflammatory pharmacological activities as well as anticancer effects (Chen et al., 2016a). As the bioactive form of ICA, ICA II is effective in ameliorating ED and pathological changes by facilitating endogenous SC differentiation in rats with BCNI (Xu et al., 2015) and attenuating the diabetes-related impairment of penile hemodynamics in diabetic rats (Zhou et al., 2012). In this study, we demonstrated that ICA II promoted the differentiation of ADSCs to SCs through the inhibition of miR-34a, and it was this initial study that discovered the positive impact of ICA II on the differentiation of ADSCs and revealed their inhibitory effect on miRNA expression. With the ICA II/miR-34a/STAT3/ADSCs/SCs pathway identified, the action mechanism of ICA II in preserving erectile function was clarified, providing potent proof for the clinical efficacy of traditional Chinese medicine at the molecular level.

miRNAs play vital roles in many fundamental biological processes through negatively regulating gene expression; indeed, they have proven to be an implication in the pathophysiological processes of ED. The miR-1, miR-200a, miR-203, and miR-206 have been validated to be up-regulated in the corpus cavernosum of rats with age-related ED, and they may also play roles via the eNOS/NO/PKG and PGE1/PKA pathways (Pan et al., 2014). miR-34a demonstrated its upside in blocking osteoporosis by inhibiting osteoclastogenesis (Krzeszinski et al., 2014) and suppressing tumor growth and metastasis through retarding cell growth (Gao et al., 2015a; Han et al., 2015). In our study, miR-34a was down-regulated by ICA II, which led to STAT3 up-regulation and the subsequent differentiation of ADSCs to SCs, contributing to preventing ED after cavernous nerve injury. miR-34a was first identified to be modulated by ICA II in the ED, and showed an adverse impact on the preservation of erectile function, providing a novel therapeutic target for ED treatment.

ADSCs originate from the vasculature of adipose tissue and share many properties with BMSCs (Chen et al., 2014) including morphology and multi-lineage differentiation potential. ADSCs have been confirmed to have therapeutic potential for cardiovascular diseases, cancers, and neurodegenerative disorders through stem cell transplantation (Chan et al., 2014; Suzuki et al., 2015). They also show great regenerative potential and provide a realistic and therapeutic strategy for ED after cavernous nerve injury (Gokce et al.,

2016). In this study, ADSCs were promoted by STAT3 to differentiate into SCs, which played a key role in neural repair and regeneration, and were devoted to preserving erectile function after cavernous nerve injury. Furthermore, the expression of nNOS increased with ADSC or ICA II treatment, which was in accordance with a previous study on the influence of ICA II on NOS (Moore and Wang, 2006; Zhou et al., 2012), reconfirming the key role of NOS in ED progression. The findings in our study implied that the impact of ICA II on NOS levels may be achieved through ADSCs, and the combined use of ICA II and ADSCs also verified this effect.

To summarize, we demonstrated that ICA II was effective in preserving erectile function after cavernous nerve injury by promoting the differentiation of ADSCs to SCs through the miR-34a/STAT3 pathway. The findings of this study highlighted the action mechanism of ICA II and laid a foundation for using ICA II scientifically in treating ED. The study also expedited the clinical application of ADSCs for ED treatment and other diseases associated with nerve injury. Due to the complex action mechanism of ICA II in different cells (Chen et al., 2016a), the mechanism of how ICA II represses the expression of miR-34a remains unclear and deserves further research in the future. With more and more studies being performed on action mechanisms, Chinese medicines may become anticipated to benefit more patients with various diseases around the world.

ACKNOWLEDGMENTS

This study was supported by grants from the Youth Science Fund of the First Affiliated Hospital of Zhengzhou University; and the Science and Technology Research Project of Henan province (NO. 172102310021).

REFERENCES

Amany, S., and Heba, K. (2013). Effect of pregabalin on erectile function and penile NOS expression in rats with streptozotocin-induced diabetes. Exp. Clin. Endocrinol. Diabetes *121*, 230-233.

Cao, Y.F., He, R.R., Cao, J., Chen, J.X., Huang, T., and Liu, Y. (2012). Drug-Drug Interactions Potential of Icariin and Its Intestinal Metabolites via Inhibition of Intestinal UDP-Glucuronosyltransferases. Evid. Based Complement Alternat. Med. *2012*, 395912.

Chan, T.M., Chen, J.Y., Ho, L.I., Lin, H.P., Hsueh, K.W., Liu, D.D., Chen, Y.H., Hsieh, A.C., Tsai, N.M., Hueng, D.Y., et al. (2014). ADSC therapy in neurodegenerative disorders. Cell Transplant *23*, 549-557.

Chen, J., Deng, S., Zhang, S., Chen, Z., Wu, S., Cai, X., Yang, X., Guo, B., and Peng, Q. (2014). The role of miRNAs in the differentiation of adipose-derived stem cells. Curr. Stem. Cell. Res. Ther. *9*, 268-279.

Chen, M., Wu, J., Luo, Q., Mo, S., Lyu, Y., Wei, Y., and Dong, J. (2016a). The Anticancer Properties of Herba Epimedii and Its Main Bioactive Componentsicariin and Icariside II. Nutrients *8, 563*.

Chen, X., Yang, Q., Zheng, T., Bian, J., Sun, X., Shi, Y., Liang, X., Gao, G., Liu, G., and Deng, C. (2016b). Neurotrophic Effect of Adipose Tissue-Derived Stem Cells on Erectile Function Recovery by Pigment Epithelium-Derived Factor Secretion in a Rat Model of Cavernous Nerve Injury. Stem Cells Int. *2016*, 5161248.

Gao, J., Li, N., Dong, Y., Li, S., Xu, L., Li, X., Li, Y., Li, Z., Ng, S.S., Sung, J.J., et al. (2015a). miR-34a-5p suppresses colorectal cancer metastasis and predicts recurrence in patients with stage II/III colorectal cancer. Oncogene *34*, 4142-4152.

Gao, S., Zheng, Y., Cai, Q., Wu, X., Yao, W., and Wang, J. (2015b). Different methods for inducing adipose-derived stem cells to differentiate into Schwann-like cells. Arch. Med. Sci. *11*, 886-892.

Gokce, A., Peak, T.C., Abdel-Mageed, A.B., and Hellstrom, W.J. (2016). Adipose tissue-derived stem cells for the treatment of erectile dysfunction. Curr. Urol. Rep. *17*, 14.

Han, Z., Zhang, Y., Yang, Q., Liu, B., Wu, J., Zhang, Y., Yang, C., and Jiang, Y. (2015). miR-497 and miR-34a retard lung cancer growth by co-inhibiting cyclin E1 (CCNE1). Oncotarget *6*, 13149-13163.

Jeong, H.H., Piao, S., Ha, J.N., Kim, I.G., Oh, S.H., Lee, J.H., Cho, H.J., Hong, S.H., Kim, S.W., and Lee, J.Y. (2013). Combined therapeutic effect of udenafil and adipose-derived stem cell (ADSC)/brain-derived neurotrophic factor (BDNF)-membrane system in a rat model of cavernous nerve injury. Urology *81*, 1108 e1107-1114.

Krzeszinski, J.Y., Wei, W., Huynh, H., Jin, Z., Wang, X., Chang, T.C., Xie, X.J., He, L., Mangala, L.S., Lopez-Berestein, G., et al. (2014). miR-34a blocks osteoporosis and bone metastasis by inhibiting osteoclastogenesis and Tgif2. Nature *512*, 431-435.

Li, H., Rokavec, M., and Hermeking, H. (2015). Soluble IL6R represents a miR-34a target: potential implications for the recently identified IL-6R/STAT3/miR-34a feed-back loop. Oncotarget *6*, 14026-14032.

Liu, T., Qin, X.C., Li, W.R., Zhou, F., Li, G.Y., Xin, H., Gong, Y.Q., and Xin, Z.C. (2011). Effects of icariin and icariside II on eNOS expression and NOS activity in porcine aorta endothelial cells. Beijing Da Xue Xue Bao *43*, 500-504.

Luo, G., Xu, B., and Huang, Y. (2017). Icariside II promotes the osteogenic differentiation of canine bone marrow mesenchymal stem cells via the PI3K/AKT/mTOR/S6K1 signaling pathways. Am. J. Transl. Res. *9*, 2077-2087.

Moore, C.R., and Wang, R. (2006). Pathophysiology and treatment of diabetic erectile dysfunction. Asian J. Androl. *8*, 675-684.

Musicki, B., Ross, A.E., Champion, H.C., Burnett, A.L., and Bivalacqua, T.J. (2009). Posttranslational modification of constitutive nitric oxide synthase in the penis. J. Androl. *30*, 352-362.

Ouyang, B., Sun, X., Han, D., Chen, S., Yao, B., Gao, Y., Bian, J., Huang, Y., Zhang, Y., Wan, Z., et al. (2014). Human urine-derived stem cells alone or genetically-modified with FGF2 improve type 2 diabetic erectile dysfunction in a rat model. PLoS One *9*, e92825.

Pan, F., Xu, J., Zhang, Q., Qiu, X., Yu, W., Xia, J., Chen, T., Pan, L., Chen, Y., and Dai, Y. (2014). Identification and characterization of the MicroRNA profile in aging rats with erectile dysfunction. J. Sex Med. *11*, 1646-1656.

Park, H., Park, H., Pak, H.J., Yang, D.Y., Kim, Y.H., Choi, W.J., Park, S.J., Cho, J.A., and Lee, K.W. (2015). miR-34a inhibits differentiation of human adipose tissue-derived stem cells by regulating cell cycle and senescence induction. Differentiation *90*, 91-100.

Shamloul, R., and Ghanem, H. (2013). Erectile dysfunction. Lancet *381*, 153-165.

Su, X., Liao, L., Shuai, Y., Jing, H., Liu, S., Zhou, H., Liu, Y., and Jin, Y. (2015). MiR-26a functions oppositely in osteogenic differentiation of BMSCs and ADSCs depending on distinct activation and roles of Wnt and BMP signaling pathway. Cell Death Dis. *6*, e1851.

Suzuki, E., Fujita, D., Takahashi, M., Oba, S., and Nishimatsu, H. (2015). Adipose tissue-derived stem cells as a therapeutic tool for cardiovascular disease. World J. Cardiol. *7*, 454-465.

Wang, L., Sanford, M.T., Xin, Z., Lin, G., and Lue, T.F. (2015). Role of Schwann cells in the regeneration of penile and peripheral nerves. Asian J. Androl. *17*, 776-782.

Wang, Y., Chu, Y., Yue, B., Ma, X., Zhang, G., Xiang, H., Liu, Y., Wang, T., Wu, X., and Chen, B. (2017). Adipose-derived

mesenchymal stem cells promote osteosarcoma proliferation and metastasis by activating the STAT3 pathway. Oncotarget *8*, 23803-23816.

Xie, Q., Wang, Z., Zhou, H., Yu, Z., Huang, Y., Sun, H., Bi, X., Wang, Y., Shi, W., Gu, P., et al. (2016). The role of miR-135-modified adipose-derived mesenchymal stem cells in bone regeneration. Biomaterials *75*, 279-294.

Xu, Y., Guan, R., Lei, H., Gao, Z., Li, H., Hui, Y., Zhou, F., Wang, L., Lin, G., and Xin, Z. (2015). Implications for differentiation of endogenous stem cells: therapeutic effect from icariside II on a rat model of postprostatectomy erectile dysfunction. Stem Cells Dev. *24*, 747-755.

Yang, R., Fang, F., Wang, J., and Guo, H. (2015). Adipose-derived stem cells ameliorate erectile dysfunction after cavernous nerve cryoinjury. Andrology *3*, 694-701.

Zhou, F., Xin, H., Liu, T., Li, G.Y., Gao, Z.Z., Liu, J., Li, W.R., Cui, W.S., Bai, G.Y., Park, N.C., et al. (2012). Effects of icariside II on improving erectile function in rats with streptozotocin-induced diabetes. J. Androl. *33*, 832-844.

Zuk, P.A. (2010). The adipose-derived stem cell: looking back and looking ahead. Mol. Biol. Cell *21*, 1783-1787.